CrystEngComm

Accepted Manuscript

ROYAL SOCIETY OF CHEMISTRY

www.rsc.org/crystengcomm

Halogen-bonded Halide Networks from Chiral Neutral Spacers

Julien Lieffrig, Arnode G. Niassy, Olivier Jeannin and Marc Fourmigué*

Institut des Sciences Chimiques de Rennes, Université Rennes 1, CNRS UMR 6226, Campus de Beaulieu, 35042 Rennes, France

Graphical abstract for Table of Content (TOC)

Chiral, ditopic, bis-iodinated molecules can form helical networks thanks to halogen bonding interactions, when co-crystallised with halide tetraalkylammonium salts.

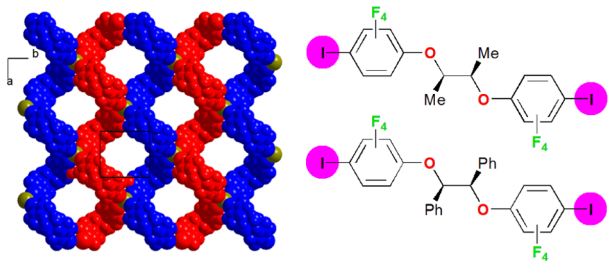

Abstract

Chiral, ditopic, halogen bond donor molecules are prepared from the reaction of C_6F_5I with three different enantiopure chiral diols, namely (*R*,*R*)-2,3-butanediol, (*R*,*R*)-hydrobenzoïne and *S*-binaphtol, with displacement of the fluorine atom *para* to the iodine atom in C_6F_5I, to give (*R*,*R*)-**1**, (*R*,*R*)-**2** and (*S*)-**3** respectively. Chiral, halogen-bonded networks with halide anions are investigated upon co-crystallisation of (*R*,*R*)-**1** with (Et_3S^+,I^-), (Et_4N^+,Br^-), (*n*-Bu_4N^+,Br^-) and (*n*-Pe_4N^+,Br^-). In the three first salts with 1:1 stoichiometry, the halide anions are coordinated by two iodine atoms, with short I•••X^- (X^- = I^-, Br^-) distances and acute (75-80°) I•••X^-•••I angles, leading to the formation of chains, eventually organized into helices around two-fold screw axes as in [(*R*,*R*)-**1**]•[Bu_4NBr]. Co-crystallisation with tetrapentylammonium bromide affords a 2:1 stoichiometry salt, [(*R*,*R*)-**1**]$_2$•[Pe_4NBr], with a four-fold coordination around the Br^- anion and the formation of a square lattice network, built out of interconnected helices.

Introduction

In the context of crystal engineering, the controlled formation of helical crystalline structures remains an attractive challenge, as such structures play a crucial role in biological[1] as well as organic or inorganic systems.[2] Accordingly, different intermolecular interactions such as metal coordination, hydrogen bonding[3] or π–π interactions[4] have been used to generate such helical supramolecular assemblies. Besides, halogen bonding[5,6,7] has been also recently established as a powerful intermolecular interaction[8] for the elaboration of complex supramolecular architectures.[9] Halogen bonding describes an attractive interaction between a Lewis base acting as halogen bond acceptor and a polarizable covalently-bound halogen atom acting as halogen bond donor, through the so-called σ-hole which develops on the halogen atom, in the prolongation of the C–X bond. This interaction is thus essentially of electrostatic nature albeit charge-transfer contributions start to play a role in the strongest halogen bonds.[10] For example, halide anions (Cl^-, Br^-, I^-) act as very efficient halogen bond acceptors, in solution[11] as in the solid state.[12] Many examples of extended anionic networks were reported incorporating neutral iodinated spacers as halogen bond donors,[13] (Scheme 1) with two, three or four halogen atoms, such as diiodoacetylene or tetraiodoethylene.[14,15] Tetrahedral CBr_4 is known to form Diamond-type structures.[16] Many other ditopic and linear molecules were used, such as α,ω-diiodoperfluoroalkanes or 1,4-diiodioperfluorobenzene.[17] Honeycomb lattices were isolated with tritopic spacers such as 1,3,5-triiodotrifluorobenzene,[18] or an

extended tris(iodoacetylene) analog,[19] with possibility thus opened for interpenetrated halide networks.[20] Besides halide anions, one can also mention thiocyanate,[21] perchlorate[22] or halometallate anions.[23]

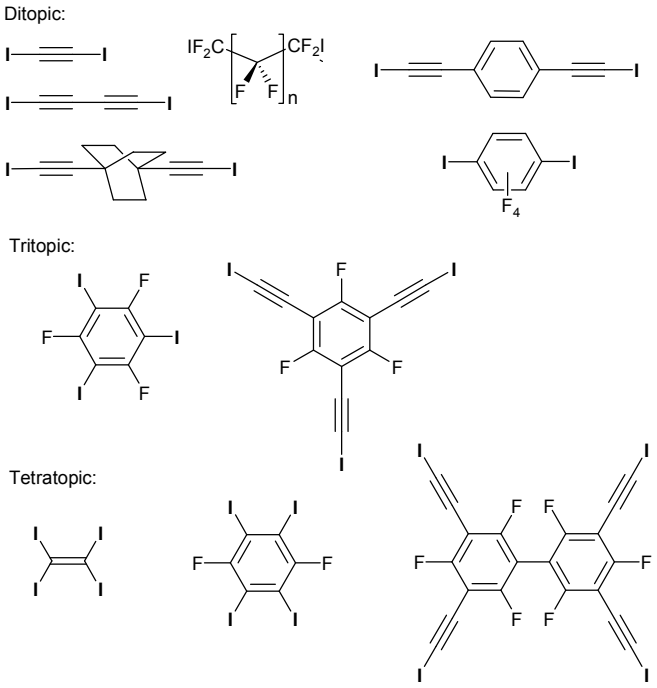

Scheme 1. Examples of di-, tri-, and tetratopic neutral molecules acting as halogen bond donor toward halide anions.

By comparison with other intermolecular interactions mentioned above, the use of halogen bonding as a crystal engineering tool in the formation of chiral, eventually helical structures has been only rarely mentioned. An earlier beautiful example is provided by the resolution of a racemic 1,2-dibromohexafluoropropane through its crystallization with (–)-sparteine hydrobromide into supramolecular helices stabilised by C–Br•••Br$^-$ halogen bond interactions.[24] Halogen bonds were also mentioned to favour the bundling of hydrogen-bonded chiral helices made out of halogen-substituted carboxylate salts of chiral amines.[3b] More recently, a chiral iodinated tetrathiafulvalene was electro-crystallised in the presence of chloride or bromide anions to afford infinite halogen-bonded chains in the chiral C222 space group.[25] In other reported examples of such networks built out of neutral di- or tetratopic halogen bond donors, the chirality or helical supramolecular organisation is most often derived from the presence of helixes of opposite chirality organized around 2_1 screw axes,[3,26] or from the spontaneous resolution of halogen bonded systems into a conglomerate of both enantiomeric crystals,[27] not only in 3D crystals, but also on 2D monolayers grown on

graphite.[28] Note also the formation of a chiral nematic phase from halogen-bonded, bent-core achiral mesogen.[29] In order to favour the formation of intrinsically chiral structures without relying only on serendipity, we decided to investigate neutral iodinated spacers with a built-in chirality, taking advantage of the availability of numerous chiral molecules in their enantiopure form. From this chiral pool, we selected appropriate precursors easily transformable into ditopic halogen bond donors, and explored their ability to crystallise with halide anions as halogen bond acceptors, toward the formation of helical halogen bonded anionic chains.

Results and Discussion

Neutral chiral spacers. Our synthetic approach to the different chiral spacers described here is based on a reaction path described earlier for achiral diols.[30,31] The S^NAr between oxygen nucleophiles and iodopentafluorobenzene displaces the fluorine atom located *para* to the iodine one, affording a variety of telechelic α,ω-di-(2,3,5,6-tetrafluoro-4-iodophenyl) derivatives. It was also demonstrated that despite the presence of a +M alkoxy substituent in the *para* position to iodine, these resulting derivatives were still effective as halogen bond donors toward neutral pyridine derivatives. We have accordingly expanded the scope of this reaction to three commercially available chiral *enantiopure* diols, namely, (*R*,*R*)-2,3-butanediol, (*R*,*R*)-hydrobenzoïne and *S*-binaphtol, as described in Scheme 2. The reaction is performed without solvent at high temperatures (160° C), with Cs_2CO_3 as base, and provide the three enantiopure compounds in good to excellent yields (60–85%).

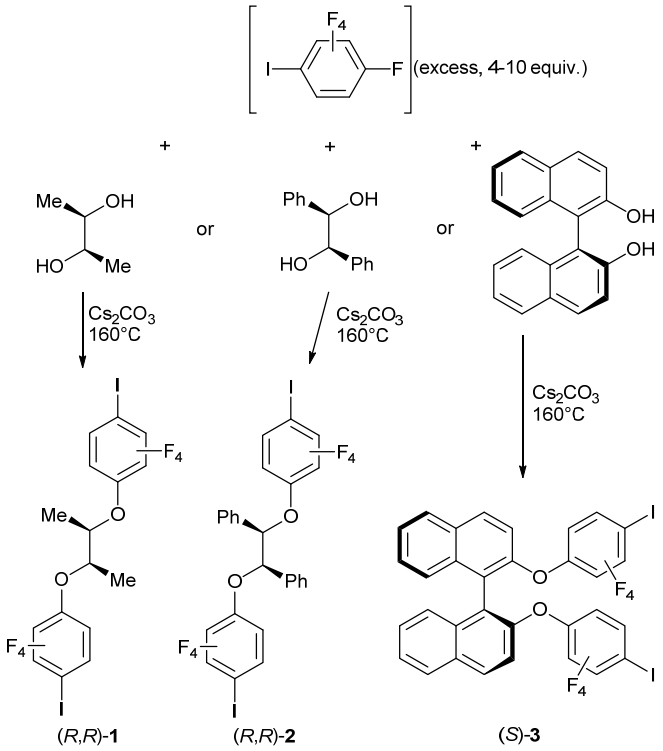

Scheme 2. Syntheses of the three enantiopure neutral halogen-bond donor molecules.

Besides usual characterizations (see Exp. Section), the three neutral molecules were also investigated by single crystal X-ray diffraction. Repeated recrystallizations of (*R*,*R*)-**1** in different solvents did not afford any good quality crystals. (*R*,*R*)-**2** crystallises in the orthorhombic system, chiral space group $P2_12_12_1$, with one molecule in general position (Figure 1a). The central C_{Ph}–C–C–C_{Ph} part adopts a *gauche* conformation, while the iodine atoms are not engaged in any specific intermolecular interactions. The binaphtol derivative (*S*)-**3** crystallises in the orthorhombic system, space group $P2_1ca$, also with one molecule in general position (Figure 1b). Note also the almost face-to-face π–π interactions between the electron-deficient iodotetrafluorophenyl and the electron-rich naphthol rings. Such π–π interactions between aryl and fluoroaryl rings are well documented as a strongly stabilizing tool in crystal engineering.[32,33] It should be stressed also here that in the two structures, the two iodine atoms are almost at opposite ends of the molecules, giving them a close-to-linear ditopic character.

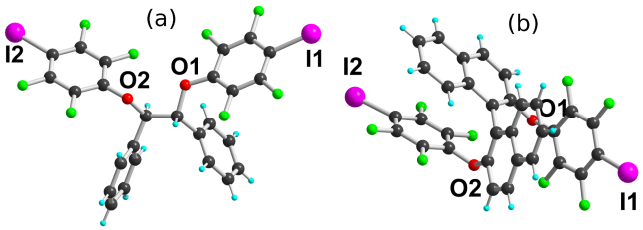

Figure 1. (a) Molecular structure of (*R*,*R*)-**2**. (b) Molecular structure of (*S*)-**3**.

Halogen bonded halide salts. Halogen-bonded networks involving halide anions as XB acceptors were successfully isolated with the butanediol derivative (*R*,*R*)-**1**. Good quality crystals were obtained with four different alkyl sulfonium and ammonium salts, namely (Et_3S^+,I^-), (Et_4N^+,Br^-), (*n*-Bu_4N^+,Br^-) and (*n*-Pe_4N^+,Br^-), from the smallest triethylsulfonium to the largest tetrapentylammonium cation. They will be described successively, with specific attention to their halogen bond characteristics as well as their supramolecular organization.

[(*R*,*R*)-**1**]•(Et_3S^+,I^-) crystallises in the monoclinic system, space group $P22_12_1$, with the Et_3S^+ cation in general position while two iodide anions and two (*R*,*R*)-**1** molecules, are located on two-fold axes, hence the resulting 1:1 stoichiometry. Considering the rotation along the central C–C bond, the two organic molecules adopt each an *anti* conformation, which gives them a V-shape (Figure 2), while the pyramidal SEt_3^+ cation is disordered on two positions. The layered structure (Figure 3) shows an alternation along *c* of cationic (SEt_3^+) and halogen bonded [(R,R)-1]•I^- anionic slabs. A projection view of one of these layers (Figure 4) shows the very acute I•••I^-•••I angles (74–76°) adopted by this structure. Such acute angles are not uncommon[12–20,34] and are probably also stabilized by the existence of important dispersion forces between the iodine atoms coming into contact.

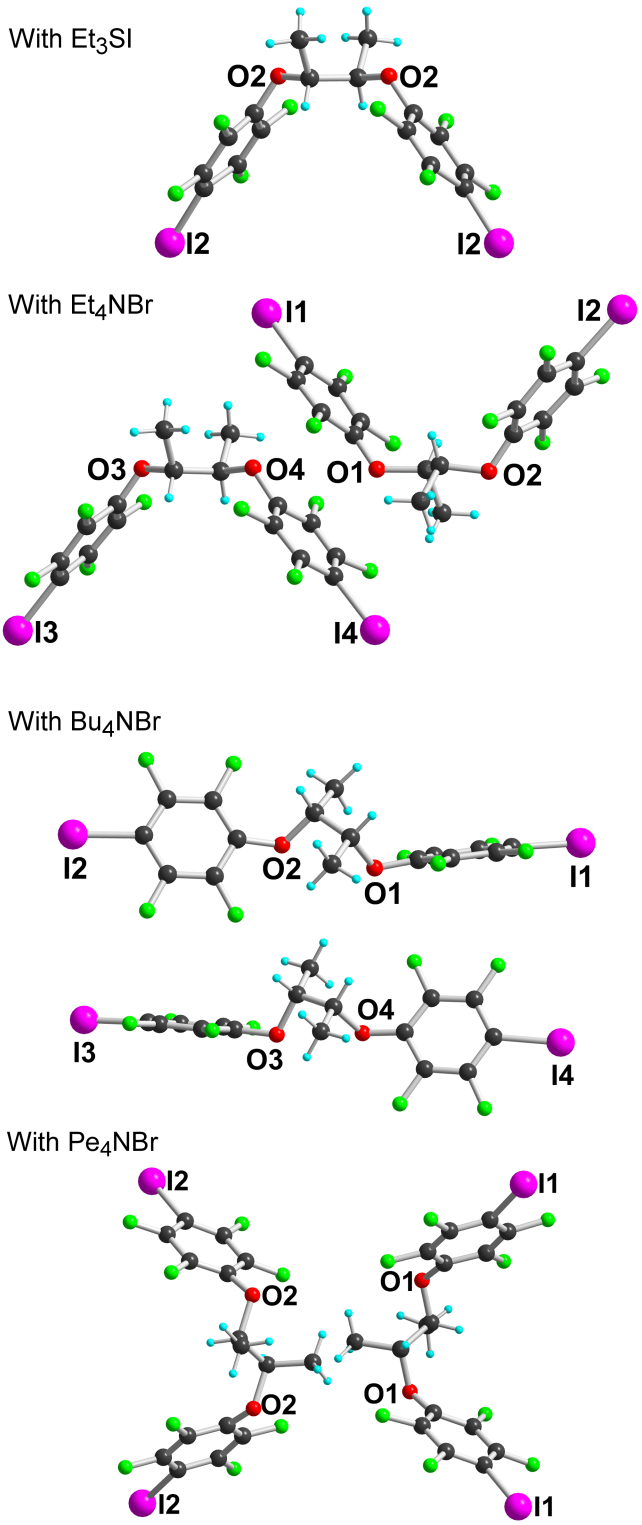

Figure 2. The different conformations adopted by (*R*,*R*)-**1** in the four different halide salts.

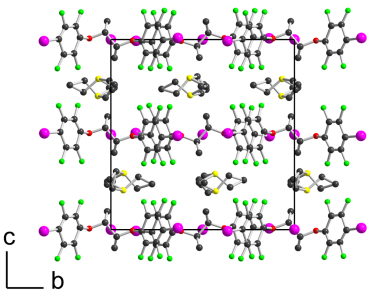

Figure 3. Projection view along the *a* axis of the unit cell of [(*R*,*R*)-**1**]•(Et_3SI), showing the segregation between the disordered SEt_3^+ cations and the complex anionic layers.

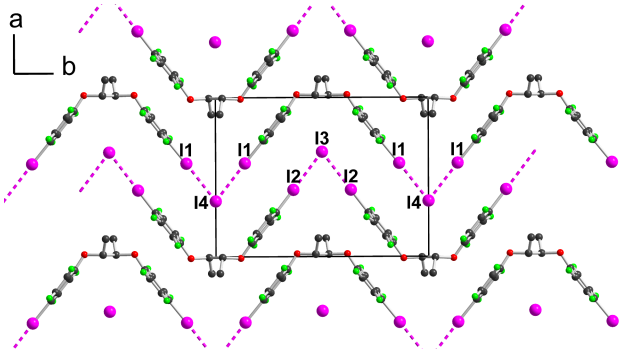

Figure 4. Projection view along *c* of one anionic layer in [(*R*,*R*)-**1**]•(Et_3SI), showing the XB interactions between the iodine atoms I(1) and I(2) of [(*R*,*R*)-**1**] and the iodide anions I(3) and I(4).

Geometrical characteristics of the I•••I^- halogen bonds collected in Table 1 confirm the important shortening when compared with the sum of van der Waals (I) and ionic (I^-) radii, as well as the strong directionality of the interactions.

Table 1. Geometrical characteristics of the halogen bonds in the three salts with [(*R*,*R*)-**1**]. Reduction parameter was calculated relative to the sum of van der Waals radius of iodine (1.98 Å) and the ionic radius of bromide (1.82 Å) or iodide (2.06 Å) anions.

Interaction	X	I•••X^- (Å)	Reduction parameter	C–I•••X^- (°)	I•••X^-•••I (°)
[(*R*,*R*)-**1**]•Et_3SI					
I(1)•••I(4)	I	3.484(1)	0.862	178.2(2)	75.59(1)
I(2)•••I(3)	I	3.475(1)	0.860	173.1(2)	74.43(1)
[(*R*,*R*)-**1**]•Et_4NBr:					
I(1)•••Br(1)	Br	3.298(6)	0.868	173.2(4)	80.25(5)
I(2)•••Br(1)	Br	3.297(6)	0.867	176.1(4)	
I(3)•••Br(2)	Br	3.266(6)	0.859	177.6(4)	79.73(5)
I(4)•••Br(2)	Br	3.250(6)	0.855	179.4(4)	
[(*R*,*R*)-**1**]•Bu_4NBr:					

I(1)•••Br(1)	Br	3.214(1)	0.846	174.1(4)	144.37(5)
I(2)•••Br(1)	Br	3.181(1)	0.837	173.4(3)	
I(3)•••Br(2)	Br	3.273(2)	0.861	175.4(3)	150.24(5)
I(4)•••Br(2)	Br	3.232(2)	0.850	172.7(3)	
[(*R*,*R*)-**1**]•Pe_4NBr:					
I(1)•••Br(1)	Br	3.319(1)	0.873	174.3(3)	77.67(2), 120.80(2)
I(2)•••Br(2)	Br	3.301(1)	0.869	175.5(3)	78.08(2), 122.74(2)

[(*R*,*R*)-**1**]•(Et_4N^+,Br^-) crystallises in the monoclinic system, space group $P2_1$, with two crystallographically independent molecules (*R*,*R*)-**1** and two crystallographically independent Et_4NBr salts. A projection view of the unit cell along *b* (Figure 5) again shows a segregation of halogen bonded [(*R*,*R*)-**1**]•Br^- anionic layers, separated from each other along the (*a*+*c*) direction by Et_4N^+ cation.

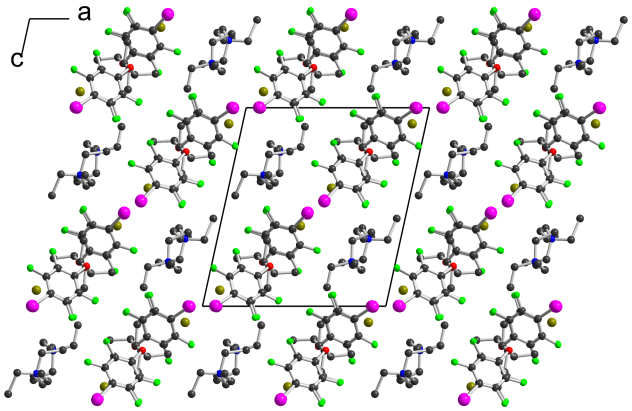

Figure 5. Projection view along *b* of the unit cell of [(*R*,*R*)-**1**]•(Et_4NBr)

Within one anionic layer, (Figure 6), the neutral molecules adopt the *anti* conformation as above (See Figure 2), and are linked to the Br^- anion to form, by translation, halogen bonded chains running along the *b*-axis, with the same acute I•••Br^-•••I angles. The two crystallographically independent chains are slightly different, with shorter and more linear interactions with the Br(2) anion (See Table 1).

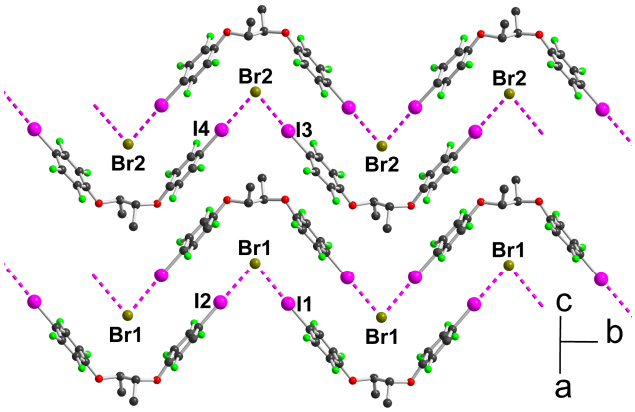

Figure 6. Projection view of one anionic layer in [(*R*,*R*)-**1**]•Et_4NBr, showing the XB interactions (pink dotted lines) with the bromide anions.

The crystal structure of the 1:1 adduct with Bu_4NBr offers another structural organization, associated now with a *gauche* conformation (see Figure 2) along the central C–C axis of [(*R*,*R*)-**1**]. Indeed, [(*R*,*R*)-**1**]•Bu_4NBr crystallises in the monoclinic system, space group $P2_12_12_1$, again with two crystallographically independent molecules and two crystallographically independent Bu_4NBr salts. The salt organizes into mixed layers incorporating the [(*R*,*R*)-**1**]•Br^- halogen-bonded chains and the Bu_4N^+ cations (Figure 7). The *gauche* conformation of the [(*R*,*R*)-**1**] molecule favours now an extended linear shape and results in a close to linear coordination around the Br^- anions, with I•••Br–•••I angles at 144.37(5) and 150.24(5)° around Br(1) and Br(2) respectively. The XB chains develop then along the two-fold screw axis running along *c*, providing the first example within these series of a helical shape given to these chains from the combination of the neutral chiral iodinated molecules and the halogen bonding to the anions.

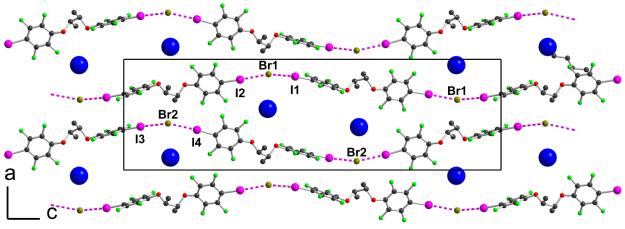

Figure 7. Projection view along *b* of the unit cell in [(*R*,*R*)-**1**]•Bu_4NBr, showing the XB interactions (pink dotted lines) with the bromide anions. The dark blue spheres are located at the nitrogen positions of the Bu_4N^+ cations

Finally, the tetrapentylammonium bromide salt crystallises in the orthorhombic P222 space group with two crystallographically independent bromide anions and two crystallographically independent cations, all of them on 222 positions, while two crystallographically independent neutral XB donor molecules (*R*,*R*)-**1** are located on a two-fold axis, hence the formulation [(*R*,*R*)-**1**]$_2$•[Pe$_4$NBr], that is now two di-iodinated molecules (*R*,*R*)-**1** for one bromide anion. The two (*R*,*R*)-**1** molecules adopt an *anti* conformation with the now characteristic V shape (Figure 2). As a consequence of this 2:1 stoichiometry, each anion is now surrounded by four iodine atoms, forming a distorted tetrahedron with I•••Br$^-$•••I angles [around Br(1)] of 77.67(2)° and 120.80(2)° (See Table 1). The halogen bonded network develops into layers alternating along the *c* axis. A projection view of one such layer (Figure 8) shows a topological square lattice structure within the (*a*,*b*) plane. These layers can also be described as parallel sets of helices interconnected through the bromide anion by halogen bonding. As shown in Figure 9, both "red" and "blue" helices running along *a* have the same left-handed (M) helicity, while those running along *b* have the same but right-handed (P) helicity. Note that the helicity observed here does not find its origin in the presence of a crystallographic 2_1 (or higher level) screw axis, but in the molecular chirality brought by the enantiopure iodinated linker.

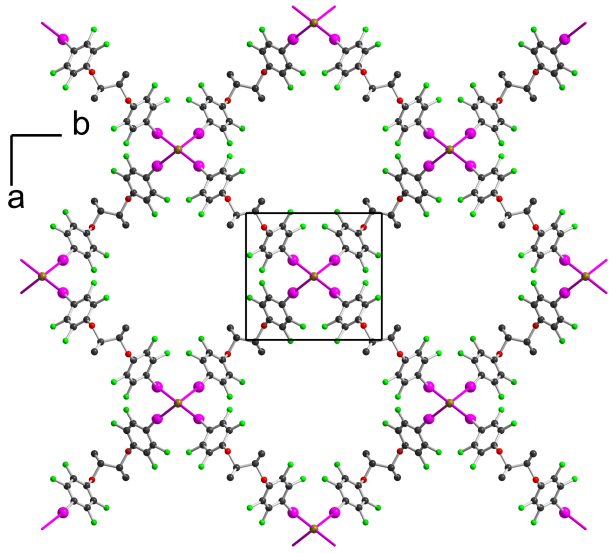

Figure 8. Projection view along *c* of one halogen bonded plane in [(*R*,*R*)-**1**]$_2$•[Pe$_4$NBr]. The tetrapentylammonium cations and hydrogen atoms have been omitted for clarity.

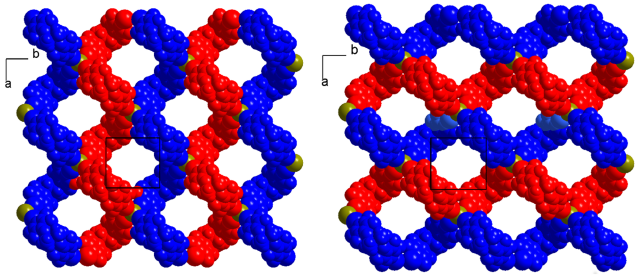

Figure 9. Projection views along *c* of one halogen bonded plane in [(*R*,*R*)-**1**]$_2$•[Pe$_4$NBr], highlighting the supramolecular helices developing along *a* (left-handed helices) or along *b* (right-handed helices). The tetrapentylammonium cations and hydrogen atoms have been omitted for clarity.

In conclusion, we have prepared original chiral, halogen bond donor, neutral molecules bearing two iodine atoms. Their conformational flexibility allows them, when co-crystallized with halide anions, to act as linear or bent bidentate spacers, allowing for the formation of chains with the Et_3S^+, Et_4N^+ and Bu_4N^+ cations, with the halide anion coordinated by two iodine atoms from two different molecules. In the tetrapentylammonium salt, a different stoichiometry, with two linkers for one bromide anion leads to a four-fold coordination around the halide, which connects helical structures running along two perpendicular directions within layers. Such anionic polymeric networks, particularly those exhibiting supramolecular helical organisation, are now being investigated as counter-ion in the electrocrystallization of π-type donor molecules such as tetrathiafulvalene derivatives,[14b,c] in order to favour the formation of chiral conducting salts,[35] of current strong interest for the observation of rare magneto-chiral anisotropy effects.[36]

Experimental section

(1R,2R)-1,2-dimethyl-1,2-bis(2,3,5,6-tetrafluoro-4-iodophenoxy)ethane: (*R*,*R*)-**1**.

Pentafluoroiodobenzene (7.1 g, 24.1 mmol) is added to a mixture of (*R*,*R*)-2,3-butanediol (0.52 g, 5.8 mmol) and Cs_2CO_3 (3.6 g, 11.0 mmol), and the whole paste is heated without solvent under Ar at 160° for 20h. After dilution with hexane and filtration on Celite®, the concentrated solution is purified by chromatography on silica gel with hexane as eluent. Recrystallization from hexane afforded (*R*,*R*)-**1** as white crystals (2.23 g). Yield: 61%. M. p. 116°C. ^{1}H NMR ($CDCl_3$, TMS, ppm) δ: 1.43 (d, 3H, CH_3), 4.60 (q, 1H, CH). ^{19}F NMR ($CDCl_3$, ppm) δ: –121.1, –153.4. ^{13}C NMR (d_6-DMSO, ppm) δ: 15.43, 67.91, 82.90, 135.99,

139.05, 142.34, 145.14, 148.30. elem. Anal. Calcd. for $C_{16}H_8F_8I_2O_2$: C, 30.12; H, 1.26%. Found: C, 30.25; H, 1.28%.

(1R,2R)-1,2-diphenyl-1,2-bis(2,3,5,6-tetrafluoro-4-iodophenoxy)ethane: (*R*,*R*)-**2** is prepared as above from (*R*,*R*)-hydrobenzoïne (0.51 g, 2.4 mmol), Cs_2CO_3 (1.54 g, 4.7 mmol) and C_6F_5I (3 mL, 22.4 mmol). Purification by chromatography on silica gel with CH_2Cl_2/hexane (1/3) as eluent. Recrystallization from hexane affords (*R*,*R*)-**2** as white crystals (1.48 g). Yield: 82%. M. p. 118°C. ^{1}H NMR ($CDCl_3$, TMS, ppm) δ: 5.61 (s, 2H, CH), 7.09-7.21 (m, 10H, Ar). ^{19}F NMR ($CDCl_3$, ppm) δ: -121.4, -152.2. ^{13}C NMR ($CDCl_3$, ppm) δ: 77.36, 88.84, 127.80, 128.53, 139.37, 134.75. Elem. Anal. Calcd. for $C_{26}H_{12}F_8I_2O_2$: C, 40.97; H, 1.59 %. Found: 41.24; H, 1.66 %.

(S)-2,2'-bis(2,3,5,6-tetrafluoro-4-iodophenoxy)-1,1'-binaphtyl: (*S*)-**3** is prepared as above from S-binaphtol (0.3 g, 1.0 mmol), Cs_2CO_3 (0.70 g, 2.1 mmol) and pentafluoroiodobenzene (3.2 g, 10.9 mmol). Silica gel chromatography and recrystallization from hexane afforded (*S*)-**3** as white crystals (0.55 g). Yield: 86%. M. p. 168°C. ^{1}H NMR ($CDCl_3$, TMS, ppm) δ: 7.15 (d, 2H, Ar), 7.25-7.4 (m, 6H, Ar), 7.83 (d, 2H, Ar), 7.92 (d, 2H, Ar). ^{19}F NMR ($CDCl_3$, ppm) δ: –121.1, –150.9. ^{13}C NMR ($CDCl_3$, ppm) δ : 77.36, 117.65, 118.92, 125.29, 125.62, 127.34, 128.27, 130.55, 130.69, 133.44. Elem. Anal. Calcd. for $C_{32}H_{12}F_8I_2O_2$: C; 46.07; H, 1.45. Found: C, 46.79 ; H, 1.67.

X-ray Diffraction Studies. Colourless crystals of the four halide salts with (*R*,*R*)-**1** were obtained as small rods by slow evaporation of mixed solutions, as detailed below. [(*R*,*R*)-**1**]•Et_3SI: a solution of (*R*,*R*)-**1** (10.8 mg, 16.9 μmol) in a 1:1 CH_2Cl_2/hexane solution (1.5 mL) is mixed with a solution of Et_3SI (4.4 mg , 17.9 μmol) in the same solvent mixture (1.5 mL). [(*R*,*R*)-**1**]•Et_4NBr: as above with Et_4NBr (7.0 mg, 22.8 μmol) in pure CH_2Cl_2. [(*R*,*R*)-**1**]•Bu_4NBr: as above with (*n*-Bu)$_4$NBr (7.0 mg, 21.7 μmol) in a 1:3 CH_2Cl_2/hexane solution. [(*R*,*R*)-**1**]$_2$•Pe_4NBr: as above with (*n*-Pe)$_4$NBr (9.5 mg, 25 μmol) in hexane solution. When collected at low temperature, single crystals were taken in a loop in oil and put directly under the N_2 stream at 150 K. Otherwise, they were glued at the end of a glass tip. Data were collected on a Bruker SMART II diffractometer with graphite-monochromated Mo-Kα radiation (λ = 0.71073 Å). Structures were solved by direct methods (SHELXS-97, SIR97)[37] and refined (SHELXL-97) by full-matrix least-squares methods,[38] as implemented in the

WinGX software package.[39] Absorption corrections were applied. Hydrogen atoms were introduced at calculated positions (riding model), included in structure factor calculations, and not refined. Restraints were introduced for the refinement of the disordered Et_3S^+ cation in [(*R*,*R*)-**1**]•Et_3SI as well as for the ends of the pentyl substituents in the Pe_4N^+ cation in [(*R*,*R*)-**1**]$_2$•Pe_4NBr. Crystallographic data are summarized in Table 2. The CIF files for each structure can be retrieved from the Cambridge Crystallographic Data Centre (CCDC) with deposition numbers CCDC 1025195-1025200, for successively (*R*,*R*)-**2**, (*S*)-**3**, [(*R*,*R*)-**1**]•Et_3SI, [(*R*,*R*)-**1**]•Et_4NBr, [(*R*,*R*)-**1**]•Bu_4NBr and [(*R*,*R*)-**1**]$_2$•Pe_4NBr.

Table 2. Crystallographic data

Compound	(*R*,*R*)-**2**	(*S*)-**3**	[(*R*,*R*)-**1**]•Et_3SI	[(*R*,*R*)-**1**]•Et_4NBr	[(*R*,*R*)-**1**]•Bu_4NBr	[(*R*,*R*)-**1**]$_2$•Pe_4NBr
Formula	$C_{26}H_{12}F_8\ I_2O_2$	$C_{32}H_{12}F_8I_2O_2$	$C_{22}H_{23}F_8I_3O_2S$	$C_{48}H_{56}Br_2F_{16}I_4N_2O_4$	$C_{32}H_{44}BrF_8I_2NO_2$	$C_{52}H_{60}BrF_{16}I_4NO_4$
FW ($g\cdot mol^{-1}$)	762.16	834.22	884.16	1696.37	960.39	1654.51
Crystal color	colourless	colourless	colourless	colourless	colourless	colourless
Cryst. size (mm)	0.87,0.43,0.38	0.26,0.16,0.03	0.31,0.14,0.12	0.40,0.38,0.23	0.42,0.28,0.17	0.27,0.11,0.01
Crystal system	orthorhombic	orthorhombic	orthorhombic	monoclinic	orthorhombic	orthorhombic
Space group	$P2_12_12_1$	$P2_1ca$	$P22_12_1$	$P2_1$	$P2_12_12_1$	P222
T (K)	293(2)	293(2)	150(2)	293(2)	150(2)	150(2)
a (Å)	8.0352(2)	8.9564(3)	11.5706(4)	13.2765(2)	12.0074(10)	9.9519(3)
b (Å)	16.1215(3)	13.3787(4)	15.5144(5)	15.9187(2)	15.2998(13)	10.6977(3)
c (Å)	20.0537(4)	23.5539(7)	16.0571(6)	14.6917(2)	41.115(3)	30.4347(10)
α (°)	90.00	90.00	90.00	90.00	90.00	90.00
β (°)	90.00	90.00	90.00	102.437(8)	90.00	90.00
γ (°)	90.00	90.00	90.00	90.00	90.00	90.00
V ($Å^3$)	2597.75(10)	2822.35(15)	2882.42(17)	3032.15(7)	7553.4(11)	3240.15(17)
Z	4	4	4	2	8	2
D_{calc} ($g\cdot cm^{-3}$)	1.949	1.963	2.037	1.858	1.689	1.696
μ (mm^{-1})	2.501	2.312	3.395	3.463	2.791	2.625
Total refls.	10107	25892	25659	58725	37334	14071
Abs. corr.	multi-scan	multi-scan	multi-scan	multi-scan	multi-scan	multi-scan
T_{min}, T_{max}	0.286, 0.387	0.648, 0.933	0.571, 0.665	0.273, 0.451	0.407, 0.622	0.714, 0.974
Unique refls.	5860	6435	6604	13706	17353	6357
R_{int}	0.040	0.0602	0.0301	0.0370	0.0495	0.0265
Unique refls. ($I > 2\sigma(I)$)	5226	3973	5063	8986	14397	5040
Refined param.	343	397	339	685	812	335
R_1 ($I > 2\sigma(I)$)	0.0475	0.0433	0.0518	0.0367	0.0823	0.0568
wR_2 (all data)	0.1269	0.1089	0.1641	0.0888	0.1856	0.1711
Flack parameter	0.06(3)	0.03(2)	0.17(7)	0.00(2)	0.10(2)	0.13(4)
Goodness-of-fit	1.069	1.021	1.134	1.128	1.172	1.162
Res. dens ($e.Å^{-3}$)	1.131, –0.821	0.465, –0.653	0.937, –1.616	0.899, –0.979	1.508, –3.200	1.339, –1.240

Acknowledgments. We thank the CDIFX (Rennes) for access to the X-ray diffractometers.

Notes and References

[1] (*a*) L. Pauling, R. B. Corey and H. R. Branson, *Proc. Natl. Acad. Sci. U. S. A.*, 1951, **37**, 205; (*b*) J. D. Watson and F. H. C. Crick, *Nature*, 1953, **171**, 737; (*c*) A. Rich and F. H. C. Crick, *Nature*, 1955, **176**, 915; (*d*) K. P. Meurer and F. P. Vögtle, *Top. Curr. Chem*., 1985, **127**, 1.

[2] (*a*) I. Sato, R. Yamashima, K. Kadowaki, J. Yamamoto, T. Shibata and K. Soai, *Angew. Chem*., 2001, **113**, 1130; (*b*) J. L. Zhou, Y. X. Wang, Y. Wang, Y. L. Song, H. G. Zheng, Y. Z. Li, L. P. Yang and X. Q. Xin, *CrystEngComm*, 2003, **5**, 62; (*c*) M. Reggelin, S. Doerr, M. Klussmann, M. Schultz and M. Holbach, *Proc. Natl. Acad. Sci. U. S. A*., 2004, **101**, 5461

[3] (*a*) S. Krishnaswamy, R. G. Gonnade, M. S. Shashidhar and M. M. Bhadbhade, *CrystEngComm*, 2010, **12**, 4184, (*b*) T. Sasaki, I. Hisaki, S. Tsuzuki, N. Tohnaia and M. Miyata, *CrystEngComm*, 2012, **14**, 5749.

[4] (*a*) V. K. Praveen, S. S. Babu, C. Vijayakumar, R. Varghese and A. Ajayaghosh, *Bull. Chem. Soc. Jpn.*, 2008, **81**, 1196; (*b*) J.-C. Xiao, J.-L. Xu, S. Cui, H.-B. Liu, S. Wang and Y.-L. Li, *Org. Lett*., 2008, **10**, 645; (*c*) F. Dumitru, Y.-M. Legrand, A. V. Lee and M. Barboiu, *Chem. Commun*., 2009, 2667.

[5] For the IUPAC definition of halogen bond, see: G. R. Desiraju, P. Shing Ho, L. Kloo, A. C. Legon, R. Marquardt, P. Metrangolo, P. Politzer, G. Resnati, and K. Rissanen, *Pure Appl. Chem*., 2013, **85**, 1711.

[6] (*a*) *Halogen Bonding: Fundamentals and Applications*; P. Metrangolo, G. Resnati, Eds.; *Structure and Bonding* **126** ; Springer-Verlag: Berlin, 2008; (*b*) G. Cavallo, P. Metrangolo, T. Pilati, G. Resnati, M. Sansotera and G. Terraneo, *Chem. Soc. Rev*., 2010, **39**, 3772; (c) P. Politzer, J. S. Murray and T. Clark, *Phys. Chem. Chem. Phys*., 2010, **12**, 7748.

[7] G. Cavallo, P. Metrangolo, T. Pilati, G. Resnati, and G. Terraneo, *Cryst. Growth Des*., 2014, **14**, 2697.

[8] W. T. Pennington, G. Resnati, and M. S. Taylor, *CrystEngComm*, 2013, **15**, 3057.

[9] (*a*) P. Metrangolo, T. Pilati, G. Terraneo, S. Biella and G. Resnati, *CrystEngComm*, 2009, **11**, 1187; (*b*) G. Cavallo, P. Metrangolo, T. Pilati, G. Resnati, M. Sansotera, and G. Terraneo, *Chem. Soc. Rev*., 2010, **39**, 3772; (*c*) F. Meyer and P. Dubois, *CrystEngComm*, 2013, **15**, 3058; (*d*) A. Mukherjee, S. Tothadi and G. R. Desiraju, *Acc. Chem. Res*., 2014, **47**, 2514.

[10] R. Cabot and C. A. Hunter, *Chem. Commun*., 2009, 2005; -(b) M. G. Sarwar , B. Dragisic, L. J. Salsberg , C. Gouliaras and M. S. Taylor, *J. Am. Chem. Soc*., 2010, **132**, 1646.

[11] (a) M. G. Chudzinski, C. A. McClary, and M. S. Taylor, J. Am. Chem. Soc., 2011, **133**, 10559; (b) M. G. Sarwar, B. Dragisic, S. Sagoo, and M. S. Taylor, *Angew. Chem. Int. Ed*., 2010, **49**, 1674.

[12] (*a*) G. Cavallo, P. Metrangolo, T. Pilati, G. Resnati, M. Sansotera and G. Terraneo , *Chem. Soc. Rev.*, 2010, **39**, 3772; (*b*) P. Metrangolo, T. Pilati, G. Terraneo, S. Biella and G. Resnati, *CrystEngComm*, 2009, **11**, 1187.

[13] (*a*) R. Weiss, M. Rechinger, F. Hampel and A. Wolski, *Angew. Chem., Int. Ed. Engl*., 1995, **34**, 441; (*b*) M. Ghassemzadeh, K. Harms and K. Dehnicke, *Chem. Ber*., 1996, **129**, 115; (*c*) M. Ghassemzadeh, K. Harms and K. Dehnicke, *Chem. Ber*., 1996, **129**, 259; (*d*) M. Ghassemzadeh, K. Harms and K. Dehnicke, *Z. Naturforsch*., 1997, **B52**, 772; (*e*) M. Ghassemzadeh, J. Magull, D. Fenske, K. Dehnicke, *Z. Naturforsch.*, 1996, **B51**, 1579.

[14] (*a*) J. D. Dunitz, H. Gehrer and D. Britton, *Acta Crystallogr*., 1972, **28**, 1989; (b) H. M. Yamamoto, J.-I. Yamaura, and R. Kato, *J. Mater. Chem*., 1998, **8**, 15; (c) H. M. Yamamoto, Y. Kosaka, R. Maeda, J. Yamaura, A. Nakao, T. Nakamura and R. Kato, *ACS Nano*, 2008, **2**, 143; (*d*) C. Lemouchi, C. S. Vogelsberg, L. Zorina, S. Simonov, P. Batail, S. Brown and M. A. Garcia-Garibay, *J. Am. Chem. Soc*., 2011, **133**, 13765.

[15] H. Bock and S. Holl, *Z. Naturforsch*. 2002, **B57**, 713.

[16] S. V. Lindeman, J. Hecht, and J. K. Kochi, *J. Am. Chem. Soc*., 2003, **125**, 11597.

[17] (a) J. Grebe, G. Geiseler, K. Harms and K. Dehnicke, *Z. Naturforsch*., 1999, **B54**, 77; (*b*) A. Abate, S. Biella, G. Cavallo, F. Meyer, H. Neukirch, P. Metrangolo, T. Pilati, G. Resnati, and G. Terraneo, *J. Fluorine Chem*., 2009, **130**, 1171.

[18] (*a*) S. Triguero, R. Llusar, V. Polo and M. Fourmigué, *Cryst. Growth Des*., 2008, **8**, 2241; (*b*) P. Metrangolo, F. Meyer, T. Pilati, G. Resnati and G. Terraneo, *Chem. Commun*., 2008, 1635.

[19] J. Lieffrig, O. Jeannin and M. Fourmigué, *J. Am. Chem. Soc*., 2013, **135**, 6200.

[20] J. Lieffrig, H. M. Yamamoto, T. Kusamoto, H. Cui, M. Fourmigué and R. Kato, *Cryst Growth Design*, 2011, **11**, 4267.

[21] (*a*) P. Cauliez, V. Polo, T. Roisnel, R. Llusar and M. Fourmigué, *CrystEngComm*, 2010, **12**, 558; (*b*) S. V. Rosokha, C. L. Stern, A. Swartz and R. Stewart, *Phys. Chem. Chem. Phys*., 2014, **16**, 12968.

[22] (*a*) A. Abate, J. Marti-Rujas, P. Metrangolo, T. Pilati, G. Resnati and G. Terraneo, *Cryst. Growth Des*., 2011, **11**, 4220; (*b*) K.-S. Shin, O. Jeannin, M. Brezgunova, S. Dahaoui, E. Aubert, E. Espinosa, P. Auban-Senzier, R. Świetlik, A. Frąckowiak, and M. Fourmigué *Dalton Trans*., 2014, **43**, 5280.

[23] J. E. Ormond-Prout, P. Smart and L. Brammer, *Cryst. Growth Des*., 2012, **12**, 205.

[24] A. Farina, S. V. Meille, M. T. Messina, P. Metrangolo, G. Resnati and G. Vecchio, *Angew. Chem. Int. Ed*., 1999, **38**, 2433.

[25] J. Lieffrig, R. Le Pennec, O. Jeannin, P. Auban-Senzier and M. Fourmigué, C*rystEngComm*, 2013, **15**, 4408.

[26] S. Muniappan, S. Lipstman and I. Goldberg, *Chem. Commun*., 2008, 1777.

[27] H. Neukirch, E. Guido, R. Liantonio, P. Metrangolo, T. Pilati and G. Resnati, *Chem. Commun*., 2005, 1534.

[28] R. Gutzler, O. Ivasenko, C. Fu, J. L. Brusso, F. Rosei and D. F. Perepichka, *Chem. Commun*., 2011, **47**, 9453.

[29] C. Präsang, A. C. Whitwood and D. W. Bruce, *Chem. Commun*., 2008, 2137.

[30] C. Guardigli, R. Liantonio, M. L. Mele, P. Metrangolo, G. Resnati, T. Pilati, *Supramol. Chem*., 2003, **15**, 177.

[31] For other examples of this reaction, see also: (*a*) J. Xu,; X. Liu,; T. Lin,; J. Huang and C. He, *Macromolecules*, 2005, **38**, 3554; (*b*) D. W. Bruce, P. Metrangolo, F. Meyer, T. Pilati, C. Präsang, G. Resnati, G. Terraneo, S. G. Wainwright and A. C. Whitwood, *Chem. Eur.* J., 2010, **16**, 9511; (*c*) L.-Y. You, S.-G. Chen, X. Zhao, Y. Liu, W.-X. Lan, Y. Zhang, H.-J. Lu, C.-Y. Cao and Z.-T. Li, *Angew. Chem. Int. Ed*., 2012, **51**, 1657; (*d*) T. Caronna, R. Liantonio, T. A. Logothetis, P. Metrangolo, T. Pilati and G. Resnati, *J. Am. Chem. Soc*., 2004, **126**, 4500; (*e*) P. Metrangolo, F. Meyer, T. Pilati, D. M. Proserpio, G. Resnati, *Chem. Eur. J*., 2007, **13**, 5765.

[32] A. Mori in *The Importance of pi- Interactions in Crystal Engineering: Frontiers in Crystal Engineering*, E. R. T. Tiekink and J. Zuckerman-Schpector Eds., John Wileys & Sons, Ltd. 2012. Chp. 7, pp. 163–185.

[33] (*a*) C. R. Patrick and G. S. Grosser, *Nature*, 1960, **187**, 1021; (*b*) G. W. Coates, A. R. Dunn, L. M. Henling, D. A. Dougherty and R. H. Grubbs, *Angew. Chem. Int. Ed. Engl*., 1997, **36**, 248; (*c*) C. Dai, P. Nguyen, T. B. Marder, A. J. Scott, W. Clegg and C. Viney, *Chem. Commun*., 1999, 2493; (*d*) S. W. Watt, C. Dai, A. J. Scott, J. M. Burke, R. L.

Thomas, J. C. Collings, C. Viney, W. Clegg and T. B. Marder, *Angew. Chem. Int. Ed*., 2004, **43**, 3061.

[34] (*a*) K. Raatikainen, G. Cavallo, P. Metrangolo, G. Resnati, K. Rissanen and G. Terraneo, *Cryst. Growth Des*., 2013, **13**, 871; (*b*) N. L. Kilah, M. D. Wise, P. D. Beer, *Cryst. Growth Des*., 2011, **11**, 4565.

[35] (a) F. Pop, P. Auban-Senzier, A. Frackowiak, K. Ptaszynski, I. Olejniczak, J. D. Wallis, E. Canadell, N. Avarvari, *J. Am. Chem. Soc*., 2013, **135**, 17176; (c) N. Avarvari, J. D. Wallis, *J. Mater. Chem*., 2009, **19**, 4061; (b) C. Réthoré, N. Avarvari, E. Canadell, P. Auban-Senzier, M; Fourmigué, J. *Am. Chem. Soc*., 2005, **127**, 5748; (c) S. Yang,, F. Pop, C.Melan, A. C. Brooks, L. Martin, P. Horton, P. Auban-Senzier, G. L. J. A. Rikken, N. Avarvari and J. D. Wallis, *CrystEngComm*, 2014, **16**, 3906.

[36] F. Pop, P. Auban-Senzier, E. Canadell, G. L. J. A. Rikken, N. Avarvari, *Nature Commun*., 2014, **5**, 3757

[37] A. Altomare, M. C. Burla, M. Camalli, G. Cascarano, C. Giacovazzo, A. Guagliardi, A. G. G. Moliterni, G. Polidori and R. Spagna, *J. Appl. Cryst.*, 1999, **32**, 115.

[38] SHELX97 - Programs for Crystal Structure Analysis (Release 97-2). G. M. Sheldrick, (1998).

[39] L. J. Farrugia, *J. Appl. Cryst.,* 1999, **32**, 837.